Supported-Catalyst Tomography

DOI: 10.1002/anie.200901308

# 3D Characterization of Gold Nanoparticles Supported on Heavy Metal Oxide Catalysts by HAADF-STEM Electron Tomography**

*J. C. González, J. C. Hernández, M. López-Haro, E. del Río, J. J. Delgado, A. B. Hungría, S. Trasobares, S. Bernal, P. A. Midgley, and José Juan Calvino**

Electron tomography has proven to be a powerful tool for the characterization of heterogeneous catalysts, and particularly of supported metal catalysts.[1–3] Of all the possible imaging modes available for electron tomography, those based on high-angle annular dark-field (HAADF) imaging in the scanning transmission electron microscope (STEM) are most suited to revealing the 3D structure of crystalline nanomaterials.[4] The compositional sensitivity of HAADF images, sometimes called *Z*-contrast images, where *Z* is the atomic number,[5] make it ideal for the investigation of heterogeneous materials with components of very different atomic numbers present. The application of HAADF-STEM to supported catalysts has focused on materials consisting predominantly of metal nanoparticles dispersed within or over light support materials, such as zeolites, alumina, or silica for which large differences between metal and support element atomic numbers contribute to a high contrast in the images.[1–4,6,7] However, to our knowledge, the use of this technique for catalysts based on heavy-element (transition metal or lanthanoid) supports has not been reported to date. Herein we focus on gold catalysts supported on a Ce-Tb-Zr mixed oxide. Currently, noble metals supported on ceria-based oxides are being studied because of their potential application as catalysts for different processes related to the production of hydrogen for fuel cells.[8,9]

A single HAADF-STEM image of a Au/$Ce_{0.50}Tb_{0.12}Zr_{0.38}O_{2-x}$ catalyst recorded during the acquisition of the series of images at various tilt angles is given in Figure 1. The contrast between the gold particles ($Z = 79$) and the oxide support (average $Z \approx 23$) is high enough to discriminate the presence of small (ca. 1 nm) particles, even in relatively thick regions of the support.

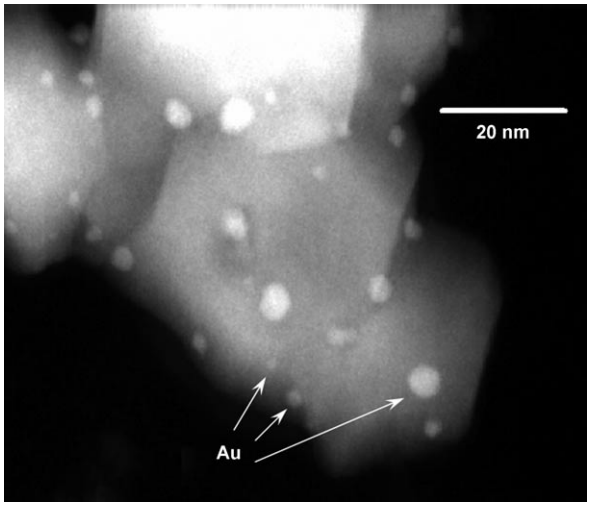


***Figure 1.*** HAADF-STEM image of the pre-reduced Au/$Ce_{0.50}Tb_{0.12}Zr_{0.38}O_{2-x}$ catalyst. The small bright areas are gold particles.

Figure 2 shows surface-rendered representations of the segmented reconstructed volumes of particles of the catalysts after pre-reduction (Figure 2a) and pre-oxidation (Figure 2b). The small volumes, colored in yellow in this figure, correspond to the high intensity areas of the HAADF images, that is, to the gold nanoparticles; regions

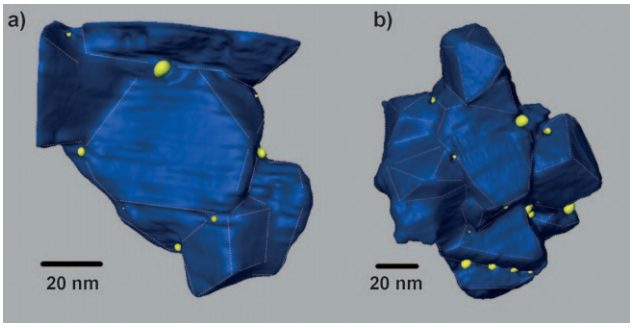


***Figure 2.*** Surface-rendered representations of the segmented reconstructed particles of the pre-reduced (a) and pre-oxidized (b) Au/$Ce_{0.50}Tb_{0.12}Zr_{0.38}O_{2-x}$ catalyst. Gold particles: yellow, mixed oxide support: blue. Dashed lines delineate the vertices of {111} facets.

[*] Dr. J. C. González, M. López-Haro, E. del Río, Dr. J. J. Delgado, Dr. A. B. Hungría, Dr. S. Trasobares, Prof. S. Bernal, Prof. J. J. Calvino
Departamento de Ciencia de los Materiales e Ingeniería Metalúrgica y Química Inorgánica, Facultad de Ciencias, Universidad de Cádiz
Puerto Real, 11510-Cádiz (Spain)
Fax: (+34) 956-016-288
E-mail: jose.calvino@uca.es
Dr. J. C. Hernández, Prof. P. A. Midgley
Department of Materials Science and Metallurgy
University of Cambridge
Pembroke Street, Cambridge, CB2 3QZ (UK)

[**] We acknowledge the financial support from Spanish MICINN/FEDER-EU (Project MAT2008-00889-NAN), and the Junta de Andalucía (Proyectos de Excelencia FQM-3994 and FQM-02433). The tomography experiments were supported by the I3 project ESTEEM (Contract Number 026019). HREM experiments were performed in SCCYT of the University of Cadiz. A.B.H. and S.T. thank the "Ramon y Cajal" Program. HAADF: high-angle annular dark-field imaging in the scanning transmission electron microscope (STEM).

Supporting information for this article is available on the WWW under http://dx.doi.org/10.1002/anie.200901308.

in blue correspond to the mixed oxide support. It should be noted that particles with diameters in the range of 1–3 nm could be successfully segmented from the reconstructions. The rounded appearance of these ultra-small particles after both types of treatment cannot be considered a reliable representation of their exact morphology because of the spatial resolution of the tomogram and the limited number of voxels (volume elements) that define the particle volume. Under these conditions, measurements such as nanoparticle volume and location can be extracted with sufficient accuracy from the reconstructions, but the individual nanoparticle morphology cannot. Recent in-situ HREM experiments carried out on $Au/TiO_2$ catalysts have revealed the occurrence of very subtle morphology changes of the particles upon changing from oxidizing to reducing environments.[10] In these 2D HREM images, gold particles had a rounded morphology under oxidizing conditions, which correlates well with our experiments herein. Very slight changes to a more facetted morphology, which are beneath the detection limit of our 3D analysis, take place under reducing atmospheres. In the same way, HREM images obtained from our samples, such as the one shown in Figure 4, also suggest a facetted shape with rounded truncations for the gold particles after both treatments; this agrees with the results observed by tomography.

A key parameter that can be analyzed from these 3D reconstructions is the surface crystallography of the support.[11,12] This issue is important to fully understand its chemical properties[13,14] and thus the catalytic behavior of the whole metal/support system. We performed crystallographic analysis on our samples and found that the surface of the $Ce_{0.50}Tb_{0.12}Zr_{0.38}O_{2-x}$ mixed oxide support is dominated by {111} facets (Figure 3). The angles between the facets observed in the reconstructed volume were measured to be close to 110°, as expected for the angle between {111} planes in a cubic crystal.[11] In fact, as the reconstructions show, the support consists mainly of octahedral crystallites of just a few nanometers in size joined to one another, possibly by twinning on {111} facets. Agglomeration of the small octahedra into the larger crystallites leads to a significant number of nanocrystal, or twin, boundaries.

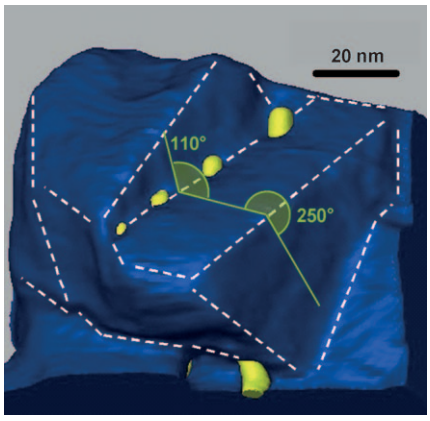


***Figure 3.*** Magnified region showing the distribution of gold nanoparticles in the reconstruction of the oxidized catalyst. The measured angle between the facets (110°) is indicated.

Another feature which can be traced from the reconstructions is the location of the gold nanoparticles on the support. Most of the metal particles are located either at the nanocrystal boundaries or at sites where a stepped surface is present (Figure 3). It is clear from the reconstruction that remarkably few metal nanoparticles are located on the facets themselves, instead preferring facet vertices and nanocrystal boundaries. This is observed for both samples, independent of the nature of the chemical treatment applied, namely reduction or oxidation.

HREM images, such as that shown in Figure 4, confirm that after treatment, the nanoparticles present in these catalysts are metallic gold with an fcc structure. The (111) planes of the gold nanoparticles grow parallel to the (111) planes of the mixed oxide. Both parallel-type (Figure 4) and twin-type orientation relationships can be found, suggesting an epitaxial relationship with the underlying support,[15] as has

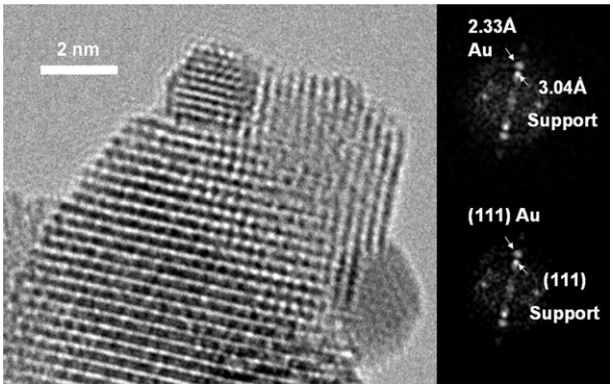


***Figure 4.*** HREM image of the oxidized catalyst. Digital diffraction patterns (right) indicate the alignment of the metal and support 111 reflections, which is consistent with an epitaxial relationship. The growth of a gold metal particle in simultaneous contact with two {111} support nanofacets can be seen. The particle at bottom right has grown onto a stepped surface.

been observed previously for gold[16] and other noble metals, such as rhodium, platinum, and palladium[17] supported on ceria-type oxides. This structural interaction between the metal particles and the support obeys the orientational interfacial fit between the {111} planes of the metal and support, and is very likely to be one of the driving forces for the peculiar distribution of the metal nanoparticles observed in this system.

The contribution of interface energy to the total energy of these small particles is expected to be important; therefore, maximizing this epitaxial interaction could provide some additional stabilization. By using a simple model, it can be calculated that for a particle with a given number of atoms, that is, with a fixed total volume, the increase in the interface contact area between a situation on a flat {111} surface to another one in which the particle sits on a {111} twin boundary amounts to about 40%. This factor could clearly contribute to a stabilization of the particle.

In summary, our study shows that quantitative 3D HAADF-STEM tomographic analysis of nanometer-sized

  

noble metal particles supported on oxides of high atomic number (Ce, Tb, and Zr) is possible. 3D reconstructed and segmented volumes yield important structural features that are not possible to determine by 2D electron microscopy. In particular, tomography reveals quantitative data about the crystallographic nature of the facets exposed by the supports and about the distribution of the supported nanoparticles on the support. In the heterogeneous catalysts we have analyzed herein, after being activated under reducing or oxidizing environments, the dispersed gold nanoparticles show a strong preferential location for nanocrystal boundaries and stepped sites of the oxide support; an epitaxial relationship between the metal and the underlying oxide support may be responsible for the predominance of this particular feature.

## Experimental Section

The 1.5% $Au/Ce_{0.50}Tb_{0.12}Zr_{0.38}O_{2-x}$ catalyst investigated was prepared by the deposition–precipitation method using a $H[AuCl_4]$ aqueous solution and urea as precipitating agent.[18] The Ce-Tb-Zr mixed-oxide support used for the preparation was a low-surface-area sample ($16\ m^2 g^{-1}$) with crystallite sizes in the range 50–100 nm. The final metal loading was confirmed by inductively coupled plasma mass spectrometry (ICP-MS) measurements. Tomography experiments were performed on a FEI Tecnai F20 field-emission gun transmission electron microscope operated at 200 kV. Data collection was carried out by tilting the specimen about a single axis using a Fischione ultrahigh-tilt tomography holder, ranging from $-72°$ to $+66°$ for pre-reduced and $-78°$ to $+68°$ and pre-oxidized samples in steps of 2°. Image acquisition was undertaken using the FEI software package Xplore3D. Alignment of the image stack and tomographic reconstructions were performed with the FEI software package Inspect 3D using the iterative routine SIRT. Surface rendering after a manual segmentation process was undertaken using Amira software. Tomographic series were recorded after submitting circa 100 mg of the fresh catalysts to two different pre-treatments: a) a 1 hour reduction treatment in flowing 5% $H_2$/Ar mixture (60 $cm^3$ STP) at 473 K, followed by a mild passivation treatment in 5% $O_2$/He starting at 233 K and being completed at 298 K; and b) an oxidation at 473 K under flowing 5% $O_2$/He mixture, also for 1 hour. High-resolution electron microscopy images were recorded in a JEOL 2010F microscope with a point resolution of 0.19 nm.

Received: March 9, 2009
Published online: June 18, 2009

**Keywords:** cerium · electron microscopy · gold · metal–support interactions · surface analysis

[1] A. J. Koster, U. Ziese, A. J. Verkleij, A. H. Janssen, K. P. de Jong, *J. Phys. Chem. B* **2000**, *104*, 9368.
[2] A. H. Janssen, C.-M. Yang, Y. Wang, F. Schüth, A. J. Koster, K. P. de Jong, *J. Phys. Chem. B* **2003**, *107*, 10552.
[3] P. A. Midgley, M. Weyland, J. M. Thomas, B. F. G. Johnson, *Chem. Commun.* **2001**, 907.
[4] J. M. Thomas, P. A. Midgley, T. J. V. Yates, J. S. Barnard, R. Raja, I. Arslan, M. Weyland, *Angew. Chem.* **2004**, *116*, 6913; *Angew. Chem. Int. Ed.* **2004**, *43*, 6745.
[5] S. J. Pennycook, D. E. Jesson, *Ultramicroscopy* **1991**, *37*, 14.
[6] Z. Li, C. Kübel, V. I. Parvulescu, R. Richards, *ACS Nano* **2008**, *2*, 1205.
[7] I. Arslan, J. C. Walmsley, E. Rytter, E. Bergene, P. A. Midgley, *J. Am. Chem. Soc.* **2008**, *130*, 5716.
[8] F. Qi, H. Saltsburg, M. Flytzani-Stephanopoulos, *Science* **2003**, *301*, 935.
[9] A. Goguet, R. Burch, Y. Chen, C. Hardacre, P. Hu, R. W. Joyner, F. C. Meunier, B. S. Mun, D. Thompsett, D. Tibiletti, *J. Phys. Chem. C* **2007**, *111*, 16927.
[10] S. Giorgio, M. Cabié, C. R. Henry, *Gold Bull.* **2008**, *41*, 167.
[11] J. C. Hernández, A. B. Hungría, J. A. Pérez-Omil, S. Trasobares, S. Bernal, P. A. Midgley, A. Alavi, J. J. Calvino, *J. Phys. Chem. C* **2007**, *111*, 9001.
[12] K. Kaneko, K. Inoke, B. Freitag, A. B. Hungria, P. A. Midgley, T. W. Hansen, J. Zhang, S. Ohara, T. Adschiri, *Nano Lett.* **2007**, *7*, 421.
[13] M. P. Yeste, J. C. Hernández, S. Bernal, G. Blanco, J. J. Calvino, J. A. Pérez-Omil, J. M. Pintado, *Chem. Mater.* **2006**, *18*, 2750.
[14] M. P. Yeste, J. C. Hernández, S. Trasobares, S. Bernal, G. Blanco, J. J. Calvino, J. A. Pérez-Omil, J. M. Pintado, *Chem. Mater.* **2008**, *20*, 5107.
[15] S. Bernal, F. J. Botana, J. J. Calvino, G. A. Cifredo, J. A. Pérez Omil y, J. M. Pintado, *Catal. Today* **1995**, *23*, 219.
[16] T. Akita, M. Okumura, K. Tanaka, M. Kohyama, M. Haruta, *J. Mater. Sci.* **2005**, *40*, 3101.
[17] S. Bernal, J. J. Calvino, J. M. Gatica, C. López-Cartes, J. M. Pintado, *Catalysis by ceria and related materials*, World Scientific—Imperial College Press, London, **2002**, Chap. 4, p. 85.
[18] R. Zanella, S. Giorgio, C. R. Henry, C. Louis, *J. Phys. Chem. B* **2002**, *106*, 7634.

  